A statistical study of the effect of preparation conditions on the structure and performance of thin film composite reverse osmosis membranes

Jaydevsinh M. Gohil[1], Akkihebbal K. Suresh*

*Department of Chemical Engineering, Indian Institute of Technology Bombay, Powai, Mumbai 400076, India,
Tel. +1 5196612111, ext. 88237; Fax: +1 5196613498; email: jay21480@yahoo.co.in (J.M. Gohil), Tel. +91 2225767240;
Fax: +91 2225726895; email: aksuresh@iitb.ac.in (A.K. Suresh)*

ABSTRACT

This work describes a statistical study of the membrane formation reaction between 1,3-phenylene diamine (MPDA) and 1,3,5-benzenetricarbonyl trichloride (TMC) on polysulfone support. The membrane performance has been characterized in terms of water flux, salt passage, and intrinsic salt permeability, and the membranes were also characterized with respect to several structural and morphological factors. The ranges within which the concentration of each monomer was varied were chosen as being relevant to industrial practice, and this is borne out by the fact that the performance of the membranes formed is within the range of practical interest. This analysis reveals that the concentrations of MPDA and TMC significantly influenced the intrinsic salt permeability, water flux, and the characteristic properties of the active polyamide layer. Polynomial models have been derived for the performance parameters using response surface methodology, and allow an identification of monomer concentrations for optimal performance of the membrane.

Keywords: Thin film composite; Response surface methodology; Polyamide; Statistical data analysis; Reverse osmosis; Membranes' structure–property

1. Introduction

Aromatic polyamide (PA) thin film composite (TFC) membrane, prepared from 1,3-phenylene diamine (MPDA) and 1,3,5-benzenetricarbonyl trichloride (or trimesoyl chloride TMC), has become the main type of reverse osmosis (RO) membrane for water desalination [1]. The reaction leading to the formation of the functional PA layer is an interfacial polycondensation (IP), which takes place between the aromatic diamine in the aqueous phase and acid chloride in the organic phase. The reaction has a complex mechanism—being a heterogeneous process it has the involvement of transport processes and chemical kinetic steps, and ionic and solution thermodynamic equilibria. The IP reaction itself is a multi-step process involving both chain extension and crosslinking in the general case, and one has to account for the phase separation processes leading to the formation of the film. In the case of TFC membranes, the properties of the support can also play a role. A certain degree of

---

*Corresponding author.

[1]Present address: Department of Chemical and Biochemical Engineering, Western University, London, Ontario, Canada N6A 5B9.

understanding of such reactions has been achieved in simpler systems such as linear polyurea in the context of microencapsulation [2,3], but the interfacial reaction in polyamide chemistry, being carried out on a support film as in the case of TFC membranes, is still poorly understood. While there have been some attempts to simulate the reaction behavior [4], sufficient experimental evidence to conclusively establish the mechanism is still lacking. The polyurea work has established the pre-eminent role of reaction kinetics, and hence, monomer concentrations, which in large part influence the kinetics in guiding the structure and properties of the film, are formed at a given temperature. It is therefore necessary that the influence of the monomer concentrations on the structure and properties of the interfacial PA layer of the TFC membranes should be clearly established, so that modeling efforts could be guided and evaluated.

In the case of PA TFC membranes, the influence of factors such as reaction time, additives, and physiochemical characteristics of base support membranes on flux and rejection are fairly well established in the literature [5–8]. However, the effect of monomer concentrations is still to be conclusively established. Ahmad and Ooi studied the effect of TMC concentration on membrane performance [6]. They observed that higher TMC concentrations lead to an enhanced rejection rate (for $CuSO_4$) and a decrease in flux, and attributed this to a reduction in pore size due to extensive crosslinking. Saha and Joshi in their study on the influence of monomer types, concluded that an increase in MPDA concentration produces membranes with more free volume and tightness within the thin film, which in turn leads to higher flux and rejection, respectively [9]. In contrast to this study, Qiu's group found that an increase in the MPDA concentration level from 0.8 to 2.4% led to a decline in the membrane flux by 34% (from 780 to $520 \, l \, m^{-2} d^{-1}$) [8]. Thus, there does not seem to be a consensus on the influence of monomer concentrations on membrane properties and performance. Another problem with many literature studies is that the performance parameters, especially the salt rejection values are often well below that of the commercial membranes, and hence, the usefulness of any conclusions arrived at for commercial membrane manufacture is questionable. The lack of consensus on the effect of monomer concentrations is not surprising, given the complexity of the process. The nature of the competition between transport and kinetic factors, for example, can be different in different concentration ranges, with a factor that is unimportant in one range becoming the controlling resistance in another.

While it is generally believed that preparation conditions influence performance through their effect on membrane structure and morphology, a further difficulty on examination of the literature is in deciphering the role of precise structural parameters in determining performance. For example, contrary to expectation, Ghosh et al. [5] found that pure water permeability of polyamide TFC membranes has a weak correlation with membrane thickness and morphology. The same attributes, however, showed a significant correlation with salt permeability [4].

This paper presents the structure–property relationship by addressing the membrane performance parameters and its structural properties. A statistical study was undertaken in order to clearly identify the influence of MPDA and TMC monomer concentrations (in absence of any additives), within the operating window of industrial relevance, on membrane function, and also to look for any correlations that exist between measurable structural attributes and performance. The approach adopted is to first establish the influence of monomer concentrations on membrane performance and structure–morphological characteristics, and then to look for correlations between structure and performance. While the first part of the study can be used to independently optimize membrane preparation conditions, the latter study should provide guidelines for understanding and modeling, as also to a choice of additives and other conditions from a consideration of how they would influence structure.

Because of the complexity of the membrane formation process, statistical methods, in conjunction with experimental designs (DoE) have been extensively used in the membrane literature to identify significant variables that influence performance and to arrive at optimal combinations of synthesis variables [10–13]. Response surface methodology (RSM) has been successfully applied to predict the optimum composition of the aqueous phase (concentrations of the monomers, catalyst, and acid acceptor) for the production of TFC membranes. In a study on polydimethylsiloxane/ceramics composite membranes [14], permeation and rejection rate were evaluated and analyzed as functions of three factors, namely polymer concentration, crosslinking agent concentration, and dip coating time, using RSM. The RSM regression model showed that polymer concentration was the most significant variable among the three. RSM, along with factorial design, has also been applied in various other areas of membrane preparation and parameter optimization [10,11,15].

This paper describes a statistical study of the membrane formation reaction between MPDA and TMC on polysulfone support. While salt rejection is commonly

employed as a measure of RO membrane performance, because of the importance of very small differences in this parameter among a series of high rejection membranes, this paper reports result in terms of salt passage. Further, as pointed out by Ghosh et al. [5], salt permeability, calculated from salt passage and water flux, is a property more intrinsic to the membrane structure than salt rejection. We therefore analyze our results with respect to this parameter. The concentration of each monomer was varied over five levels with three replicate syntheses at each combination. The range of concentrations was chosen based on patent and published literature [16–18]. In an effort to examine the correlations between structural attributes and functional responses, the membranes were also characterized for membrane thickness, surface morphology and roughness, surface charge (zeta potential), surface hydrophilicity, and microstructural morphology. Subsequently, the results were statistically analyzed by a multivariable analysis of variance (ANOVA) with repetition and RSM with factorial design was used to fit polynomial models, and to understand the effect of the two concentrations chosen as independent variables, on the responses.

2. Theory: statistical data analysis

Details of RSM, and the concepts of statistical experimental design, regression modeling techniques, and elementary optimization methods on which it relies are available in standard works on statistical analysis, and only brief details will be given here. The central concept of ANOVA, which compares, in a statistical sense, the effect of the factors chosen for study with that of the experimental error, and hence enable conclusions to be drawn about the significance of such factors. ANOVA can not only be used to analyze the main effects of the variables, but also their interaction effects when we have more than one independent variable [19]. RSM provides, based on ANOVA, for a visualization of the effect of parameters through the response surface contours [20], and also quantitative relationships for the system responses as functions of the input independent variables. In the first step, RSM finds an approximation for the true functional relationship. For k input variables $X_1, X_2, \ldots, X_k$ for example, a first-order model for the response Y can be written as follows:

$$Y = \beta_0 + \beta_1 X_1 + \beta_2 X_2 + \cdots + \beta_k X_k + \varepsilon \quad (1)$$

where the coefficients β_k show the linear effect of the kth factor coefficients and ε is the error in Y.

If there is a curvature in the system response, then a polynomial of higher degree is used; second- or third-order models such as the ones below are common:

$$Y = \beta_0 + \sum_{i=1}^{k} \beta_i X_i + \sum_{i=1}^{k} \beta_{ii} X_i^2 + \sum_{i=1}^{k-1}\sum_{i<1}^{k} \beta_{ij} X_i X_j + \varepsilon \quad (2)$$

$$Y = \beta_0 + \sum_{i=1}^{k} \beta_i X_i + \sum_{i=1}^{k} \beta_{ii} X_i^2 + \sum_{i=1}^{k} \beta_{iii} X_i^3 + \sum_{i<1}\sum_{i=1}^{k} \beta_{ij} X_i X_j + \sum_{i<j}\sum_{j<k}\sum_{i=1}^{k} \beta_{ijk} X_i X_j X_k + \varepsilon \quad (3)$$

where β_0 is the constant, β_i are the coefficients of the linear terms, β_{ii} are quadratic term coefficients, and β_{iii} cubic term coefficients. B_{ij} and β_{ijk} are cross-product term coefficients and embody the interactions. X_i and X_j represents the coded levels of the independent variables.

3. Experimental

3.1. Materials and membrane preparation

The polysulfone (PSF) base support membrane was supplied by Dow Chemicals (USA). MPDA and TMC were purchased from Aldrich Chemicals Co. (USA). Hexane and Sodium carbonate were procured from Merck & Co. (USA). All the chemicals were used without further purification. In order to benchmark the performance and characteristics of the membranes prepared in the laboratory against commercial desalination membranes, the commercial membrane BW30 (used for brackish water desalination) was used. This was also supplied by Dow Chemicals (USA).

Fresh TMC and MPDA solutions (concentrations as shown in Table 1) were prepared in hexane and Milli-Q water, respectively. To prepare the TFC membranes, the PSF support membrane stored in water containing isopropanol was wiped, dried, and

Table 1
Actual and coded variable factors considered for experimental design

	Levels				
	Lowest	Low	Centre	High	Highest
Factors (w/v%)	−1	−0.5	0	0.5	1
(X_1) [TMC]	0.05	0.1	0.15	0.2	0.3
(X_2) [MPDA]	1	1.5	2	2.5	3

contacted with MPDA solution for 3 min. The excess solution was drained for 8–10 min and the membrane was contacted with the TMC solution in hexane for 50–60 s. These parameters were arrived at after some initial trial and error. After draining the TMC solution for 15 s, the membrane was heat treated at 80°C for 5 min. The resulting TFC membrane (with the polyamide formed on top of PSF) was first washed with hot water at 50°C for 3 min and subsequently washed with a solution of Na$_2$CO$_3$ (0.2 wt.%) for 3 min. The membrane was finally washed with de-ionized water and stored in a closed container.

3.2. Membrane characterization

The membranes were characterized with respect to thickness of the PA layer (and its distribution), surface charge, contact angle, and surface morphology. Following the above procedure of membrane preparation, a separate set of membranes was prepared in order to make it feasible to characterize the membrane with respect to all the properties of interest, from a single piece.

A Surface profiler (Dektak 150 Stylus Profiler, Veeco Instruments Inc., USA) was employed to measure the thickness of the isolated PA thin film. The method for PA film isolation and deposition onto glass slide from composite membrane was followed as developed in a companion study. A diamond stylus (12.1 μm diameter) was moved across the membrane, starting from the surface of the glass slide and moving across the thin film, the contact force being 9.8×10^{-6} N. The variation in the vertical position of the stylus was recorded as a function of its horizontal position as the stylus was moved.

The surface zeta potential of TFC membranes was determined using ZetaCAD (Version 2.0.1, CAD Instruments, France). The streaming potential was determined with 10-mM NaCl solution at unadjusted pH (5.8). All the membranes were soaked in a 10-mM NaCl solution for 24 h before measurement. The electrolyte solution was passed through the membrane cell in both directions for 30 min to equilibrate the membrane surface. The measurement was performed at a pressure of 500 mbar at 25°C. The experiment was repeated until a constant value of zeta potential was attained.

A contact angle goniometer (DIGIDROP, GBX Instruments DS Model, France) was used for measurement of contact angle on the membrane surface, in order to gain an appreciation of the hydrophilicity of the membrane. The membrane samples were dried overnight in a desiccator and attached to a glass slide. In the equilibrium sessile drop technique that was followed, a steady contact angle was reached between 30 and 120 s

after contact was established between the water droplet and the membrane surface. The contact angle was measured at five different locations for each membrane.

The surface morphology of membranes was examined using field emission gun-scanning electron microscopy (FEG-SEM, JEOL JSM-7600F). The dried membrane samples were first sputter coated (JFC-1800) with a uniform layer of platinum to a thickness of about 10 nm to avoid charging. The scanning electron microscopy (SEM) images were taken at an accelerating voltage of 10 kV.

Quantitative aspects of the surface morphology were determined using atomic force microscopy (AFM). Images were taken in the tapping mode using Nanoscope IV scanning probe microscope equipped with a 6642J scanner (Digital Instruments Multimode, Singapore). A silicon nitride probe cantilever (spring constant 40 N m^{-1}, length 115–135 μm, and nominal tip radius of curvature 8–10 nm) was used at a resonance frequency of 300 kHz.

3.3. Performance evaluation

Desalination performance of the TFC membranes was determined using a flat-sheet cross-flow permeation cell (Sterlitech Corporation, USA) with an active area of 42 cm^2. The feed solution of 2,000-ppm NaCl was passed at 1.55 MPa. The membrane permeate was collected after 1 h to calculate volumetric permeate flux rate (J_v). The salt concentrations in the permeate (C_p) and the feed (C_f) were measured using a previously calibrated conductivity meter. The salt passage (R_p) through the membrane was calculated as follows:

$$R_p = C_p/C_f \tag{4}$$

While salt passage (R_p) (or rejection) is important as an overall indicator of membrane performance, it depends on membrane characteristics as well as the total flux passing through the membrane. An intrinsic measure of the goodness of the membrane for desalination can be provided by salt permeability, which for dilute solutions used here, can be calculated as:

$$B = J_v R_p/(1 - R_p) \tag{5}$$

Since, it is usual to find that the conditions which improve water flux also increase salt passage as well. Eq. (5) shows an additional advantage of employing salt passage in preference to salt rejection. Further, trends in salt passage are accentuated and made easier to interpret when cast in terms of the intrinsic salt permeability, *B*.

Table 2
Experimental results on water flux (J_v), salt passage (R_p), and calculated intrinsic salt permeability (B) for different combinations of X_1 and X_2

| Factor (X_1): [TMC] (w/v%) | Factor (X_2): [MPDA] (w/v%) | | | | | | | | | | | | | | |
| | 1 | | | 1.5 | | | 2 | | | 2.5 | | | 3 | | |
	R_p	B	J_v	R_p	B	J_v	R_p	B	J_v	R_p	B	J_v	R_p	B	J_v
0.05	7.40	0.348	43.52	2.40	0.161	65.51	3.80	0.228	57.75	2.00	0.153	75.00	4.8	0.563	111.57
0.05	7.39	0.357	44.79	2.48	0.127	50.00	2.80	0.207	71.76	2.80	0.222	76.97	3.40	0.298	84.72
0.05	3.95	0.168	40.74	3.79	0.222	56.25	2.70	0.189	67.94	3.31	0.250	72.92	4.83	0.513	101.16
0.10	5.89	0.240	38.43	4.65	0.238	48.73	2.80	0.155	53.82	2.70	0.181	65.39	2.60	0.274	102.66
0.10	5.38	0.193	33.91	3.13	0.155	48.03	1.63	0.103	62.27	2.42	0.169	68.17	3.80	0.327	82.75
0.10	3.58	0.143	38.54	2.37	0.140	57.64	1.56	0.078	49.31	2.60	0.200	74.88	4.10	0.418	97.80
0.15	4.34	0.160	35.30	2.70	0.121	43.52	2.40	0.123	50.00	2.54	0.205	78.59	2.70	0.256	92.36
0.15	4.22	0.161	36.46	3.32	0.127	36.92	2.90	0.155	51.97	2.80	0.183	63.54	2.90	0.223	74.54
0.15	4.41	0.177	38.43	1.9	0.084	43.52	1.90	0.091	47.22	2.82	0.201	69.21	3.10	0.275	85.88
0.20	2.80	0.097	33.56	2.65	0.101	36.92	2.70	0.123	44.33	2.80	0.133	46.18	2.30	0.159	67.71
0.20	5.89	0.230	36.81	2.87	0.098	33.22	2.43	0.118	47.34	2.40	0.128	51.97	2.90	0.198	66.44
0.20	2.52	0.085	32.75	2.79	0.121	42.01	2.59	0.117	43.87	2.79	0.144	50.00	2.60	0.179	67.01
0.30	3.70	0.116	30.09	3.02	0.086	27.55	2.60	0.074	27.78	1.26	0.051	39.70	1.55	0.082	51.85
0.30	4.05	0.108	25.69	2.48	0.074	28.94	0.99	0.031	30.79	1.87	0.068	35.65	2.17	0.128	57.64
0.30	3.87	0.112	27.89	2.75	0.080	28.24	1.79	0.053	29.28	1.56	0.060	37.73	1.86	0.104	54.75

Note: R_p is salt passage (%), B is the intrinsic salt permeability (μm s^{-1}); J_v is the water flux (10^7 m^3 m^{-2} s^{-1}).

3.4. Experimental design

A factorial design was adopted in the present study, with the two factors X_1 (TMC concentration) and X_2 (MPDA concentration), each taken at five levels. A two-way ANOVA was used to analyze the statistical significance of the factors and their interactions. The levels of variables used in this study are shown in Table 1. With three replicates for each combination of factors X_1 and X_2, in all 75 experimental fabrications of the membrane were carried out for the performance studies. Table 2 records, for all the experiments, the responses R_p, B, and J_v. Seventy five experiments were performed in random order.

The experimental variables and the responses shown in Tables 1 and 2 were used to determine the regression models using Design-Expert Version 8.0.3.1 software (Trial version, from Stat-Ease, Inc.). The response surface and the contour plots were generated using the same software.

4. Results and discussion

4.1. Analysis of membrane performance responses

Table 2 records the complete details of salt passage, intrinsic salt permeability, and water flux in all the experiments. The salt passage values for our membranes ranged from 0.99% to 7.4% and thus the best membranes were comparable to the commercial BW30 membrane (Dow Chemicals, USA), for, which the salt passage was 2.6% as measured under the same conditions in our laboratory. While the water flux for our membranes, which was in the range of 25.7×10^{-7} – 111.6×10^{-7} m^3 m^{-2} s^{-1}, was a little lower (under the same conditions, BW30 gave a water flux of about 136.11×10^{-7} m^3 m^{-2} s^{-1}); we have shown in a recent work that the water flux can be improved without affecting the salt rejection by the use of controlled amounts of additives such as dimethyl sulfoxide [21]. The characteristics of the membrane such as thickness, contact angle, and zeta potential were also comparable to those of BW30, while the roughness of the present membranes was higher. This could, at least in part, be owing to the differences in preparation method between the laboratory and the industry. The reacting solutions are stationary in the (batch mode) laboratory synthesis, while in industrial manufacture, the support membrane would be continuously moving through the reactive solutions during the reaction, as a result of which the surface experiences a fluid shear.

ANOVA was applied to test the significance of the two experimental variables, concentrations of TMC ([TMC]) and MPDA ([MPDA]), on the responses, salt passage (R_p), intrinsic salt permeability (B), and water flux (J_v). Significance of the factors was determined based on a comparison between the calculated F-value and the tabulated value at a chosen level of significance (usually 0.95), or tabulated p-value (also termed

Table 3
ANOVA table for response (a) R_p, (b) B, and (c) J_v

Source	SS	DF	MS	F-value	p-value	Prob. > [a]F
(a) R_p (%)						
X_1 treatments	18.03	4	4.51	7.27	0.0001	2.56
X_2 treatments	49.99	4	12.50	20.16	6.0E-10	2.56
$X_1 X_2$ interaction	12.17	16	0.76	1.22	0.278	1.85
Error	30.87	50	0.62			
Total	111.1	74				
(b) B (µm s^{-1})						
X_1 treatments	0.290	4	0.073	30.59	6.86E-13	2.56
X_2 treatments	0.202	4	0.051	21.30	2.66E-10	2.56
$X_1 X_2$ interaction	0.099	16	0.006	2.60	5.11E-03	1.85
Error	0.119	50	0.002			
Total	0.710	74	l			
(c) J_v (m^3 m^{-2} s^{-1})						
X_1 treatments	9.78E-11	4	2.45E-11	83.29	1.77E-21	2.56
X_2 treatments	1.78E-10	4	4.45E-11	151.54	2.70E-27	2.56
$X_1 X_2$ interaction	1.62E-11	16	1.01E-12	3.45	4.07E-04	1.85
Error	1.47E-11	50	2.94E-13			
Total	3.07E-10	74				

SS: sum of squares; DF: degree of freedom; MS: mean square.
[a]The value of F_{crit}: [a]$F_{0.999}(4,50) = 5.46$　$(p = 0.001)$;　$F_{0.99}(4,50) = 3.72$　$(p = 0.01)$;　$F_{0.975}(4,50) = 3.05$　$(p = 0.025)$;　$F_{0.95}(4,50) = 2.56$　$(p = 0.05)$; $F_{0.999}(16,50) = 3.14$　$(p = 0.001)$;　$F_{0.99}(16,50) = 2.38$　$(p = 0.01)$;　$F_{0.975}(16,50) = 2.08$　$(p = 0.025)$; and $F_{0.95}(16,50) = 1.85$　$(p = 0.05)$.

"Prob. > F" value). If the calculated F-value turns out greater than tabulated value, then the corresponding factor may be deemed significant at the chosen level of significance. The details, for response R_p, B, and J_v are presented in Table 3. As seen from the table, TMC and MPDA treatments showed a significant effect on responses R_p, B, and J_v since $F > F_{0.95}$ (some additional F_{crit} values at other levels of significance are also indicated below the table for comparison). While the interaction effect between TMC and MPDA treatments ($X_1 X_2$) was not significant for salt passage at this level of significance, it was significant for B, which as noted above, is a more fundamental property of the membrane. While most studies of this nature concentrate on salt rejection and water flux, it is clearly the fundamental attributes of water and salt permeability that one should address if the objective is to arrive at optimal values of the synthesis parameters.

When the interaction effect is significant, further test of significance is necessary [22]. Table 4 summarizes the simple main effect of [TMC] at each level of [MPDA] for the three responses of interest. Again, while the results for salt passage show the simple effect of [TMC] to be significant only at the extreme values of [MPDA], the results for intrinsic salt permeability show it to be significant at all except one level of [MPDA]

(even at that level, the F-value of 2.31 at [MPDA] = 1.5 w/v% was only marginally below the critical value $F_{0.95} = 2.56$). For flux rate, the calculated F-values indicate that the simple effect of TMC treatment for all MPDA treatment levels was significant at 0.05 level of significance. The trend for the simple mean effect of TMC for intrinsic salt permeability, at different [MPDA] levels, was 1.5% < 2% < 2.5% < 1% < 3%, while for water flux, it was 1% < 1.5% < 2% < 2.5% < 3%.

Table 5 outlines the simple main effect of MPDA treatment at different levels of [TMC]. It is seen that trends in salt passage are clear and sharp when examined in terms of those in B, B shows regular trends that are easier to rationalize than salt passage. The effect decreased uniformly as [TMC] increased, and was not significant at [TMC] values higher than 0.2. The analysis for flux rate shows the simple main effect of MPDA treatment to be significant for all the treatment levels of TMC. The trend in response obtained shows the effect to be higher at the lower three values of [TMC] (0.05, 0.1, and 0.15 w/v%) as compared to that at the higher two values (0.2 and 0.3 w/v%).

Overall, it is seen from the results that a low value of [TMC] and a high value of [MPDA] were conducive to producing high flux membranes. The effect of [TMC] on water flux was more pronounced at larger

Table 4
ANOVA for simple effect of factor X_1 ($n = 3$)

Source	SS	DF	MS	[a]F-value
(a) R_p (%)				
SS X_1 for 1 (w/v%) of X_2	12.54	4	3.13	5.06
SS X_1 for 1.5 (w/v%) of X_2	1.02	4	0.25	0.41
SS X_1 for 2 (w/v%) of X_2	3.14	4	0.78	1.27
SS X_1 for 2.5 (w/v%) of X_2	2.95	4	0.74	1.19
SS X_1 for 3 (w/v%) of X_2	10.55	4	2.64	4.25
Within treatment (error)	30.87	50	0.62	
(b) B (μm s^{-1})				
SS X_1 for 1 (w/v%) of X_2	0.057	4	0.014	6.03
SS X_1 for 1.5 (w/v%) of X_2	0.022	4	0.005	2.31
SS X_1 for 2 (w/v%) of X_2	0.037	4	0.009	3.87
SS X_1 for 2.5 (w/v%) of X_2	0.045	4	0.011	4.70
SS X_1 for 3 (w/v%) of X_2	0.229	4	0.057	24.09
Within treatment (error)	0.119	50	0.002	
(c) J_v (m^3 m^{-2} s^{-1})				
SS X_1 for 1 (w/v%) of X_2	3.57E-12	4	8.91E-13	3.04
SS X_1 for 1.5 (w/v%) of X_2	1.58E-11	4	3.95E-12	13.46
SS X_1 for 2 (w/v%) of X_2	2.17E-11	4	5.43E-12	18.50
SS X_1 for 2.5 (w/v%) of X_2	3.10E-11	4	7.74E-12	26.37
SS X_1 for 3 (w/v%) of X_2	4.19E-11	4	1.05E-11	35.70
Within treatment (Error)	1.47E-11	50	2.94E-13	

[a]The value of F_{crit}: [a]$F_{0.99}(4,50) = 3.72$ ($p = 0.01$); $F_{0.975}(4,50) = 3.05$; and $F_{0.95}(4,50) = 2.56$ ($p = 0.05$).

Table 5
ANOVA for simple effect of factor X_2 ($n = 3$)

Source	SS	DF	MS	F-value
(a) R_p (%)				
SS X_2 for 0.05 (w/v%) of X_1	26.36	4	6.59	10.63
SS X_2 for 0.1 (w/v%) of X_1	14.98	4	3.74	6.04
SS X_2 for 0.15 (w/v%) of X_1	6.99	4	1.75	2.82
SS X_2 for 0.2 (w/v%) of X_1	2.89	4	0.72	1.17
SS X_2 for 0.3 (w/v%) of X_1	10.94	4	2.73	4.41
Within treatment (error)	30.87	50	0.62	
(b) B (μm s^{-1})				
SS X_2 for 0.05 (w/v%) of X_1	0.160	4	0.04	16.89
SS X_2 for 0.1 (w/v%) of X_1	0.084	4	0.021	8.87
SS X_2 for 0.15 (w/v%) of X_1	0.039	4	0.01	4.11
SS X_2 for 0.2 (w/v%) of X_1	0.009	4	0.002	0.948
SS X_2 for 0.3 (w/v%) of X_1	0.008	4	0.002	0.878
(c) J_v (m^3 m^{-2} s^{-1})				
SS X_2 for 0.05 (w/v%) of X_1	5.29E-11	4	1.32E-11	45.04
SS X_2 for 0.1 (w/v%) of X_1	5.67E-11	4	1.42E-11	48.28
SS X_2 for 0.15 (w/v%) of X_1	4.90E-11	4	1.22E-11	41.69
SS X_2 for 0.2 (w/v%) of X_1	1.99E-11	4	4.97E-12	16.92
SS X_2 for 0.3 (w/v%) of X_1	1.57E-11	4	3.93E-12	13.39
Within treatment (error)	1.47E-11	50	2.94E-13	

[MPDA] values, and the effect of [MPDA], at lower values of [TMC]. While the results on salt passage were more difficult to interpret, results on B showed clearer trends, with higher values of [TMC] being the better choice for low values of B (the effect was generally more pronounced at larger values of [MPDA]). As for the value of [MPDA] for targeting low B, an intermediate range seemed to be better than either extremes in the range studied. The results, thus show the pitfalls in focusing on salt rejection as a response as compared to intrinsic salt permeability, if the objective is to optimize synthesis conditions.

4.1.1. The fitting of response surface models

To visualize the shape and contours of the response surfaces, and to fit appropriate regression models to facilitate quantitative optimization, the variable factor levels and responses (B, R_p, and J_v) shown in Tables 1 and 2 were fed into the Design Expert Version 8.0.3.1 software. To fit a good model, tests of significance for the regression model and for the individual model coefficients, as well as a test for lack-of-fit have to be carried out [23]. Examination of the fit summary output revealed that a cubic model was statistically significant for salt passage and intrinsic salt permeability, while a quadratic model was statistically significant for the flux rate. In view of the discussion above, only results for intrinsic salt permeability and water flux are discussed further. A backward elimination procedure was adopted (with an adherence to the principle of hierarchy) to eliminate the insignificant terms in order to obtain an improved

model. In this procedure, from the full cubic model, the term that is least significant—that is, the one with the largest p-value—was removed and the model was refitted. Each subsequent step removes the least significant term in the model until all remaining variables have individual p-values smaller than some value, such as 0.05 or 0.10, but hierarchical terms are retained. The backward elimination procedure is suggested in the literature as being less adversely affected by any correlation among the variables. For the sake of brevity, only details of the reduced model are presented and discussed.

Table 6 shows the ANOVA results for the reduced cubic model for intrinsic salt permeability. The model F-value of 34.33 implies that the model is significant. The p-value in the last column indicates that there is only a 0.01% chance that a model F-value this large could occur due to noise. Values of "Prob > F" less than 0.05 indicate that the model terms are significant. The "Lack of Fit F-value" of 0.90 implies that the Lack of Fit is not significant relative to pure error—the associated P-value shows that there is a 58.24% chance that a lack of fit F-value this large could occur due to noise. The ranking of the significant model terms was: quadratic effect of [MPDA] (X_2^2) > simple effect of [TMC] (X_1) > two-level interaction of [TMC] and quadratic effect of [MPDA] ($X_1X_2^2$) > two-level interaction of [TMC] and [MPDA] (X_1X_2). The calculated R^2 value shows that about 78.2% of the observed variation is accounted for the model [19]. This value is also in reasonable agreement with the adjusted R^2 of 0.7592. The value of adequate precision of 22.825 is satisfactory in terms of a signal-to-noise ratio, since a value >4 indicates an

Table 6
ANOVA table (partial sum of squares) for response surface reduced cubic model (Response: B)

Source	SS	DF	MS	F-value	p-value
Model	0.555246	7	0.079321	34.33368	<0.0001 significant
X_1	0.040459	1	0.040459	17.51271	<0.0001
X_2	0.001231	1	0.001231	0.53291	0.4679
X_1X_2	0.031288	1	0.031288	13.54294	0.0005
X_1^2	0.008499	1	0.008499	3.67885	0.0594
X_2^2	0.113212	1	0.113212	49.00331	<0.0001
$X_1X_2^2$	0.033899	1	0.033899	14.67301	0.0003
X_2^3	0.001503	1	0.001503	0.650453	0.4228
Residual	0.15479	67	0.00231		
Lack of Fit	0.036124	17	0.002125	0.89535	0.5824 not significant
Pure Error	0.118666	50	0.002373		
Cor Total	0.710036	74			
Standard deviation	0.05		R^2	0.7820	
Mean	0.17		Adjusted R^2	0.7592	
C.V.%	28.13		Predicted R^2	0.7078	
PRESS[a]	0.21		Adequate precision	22.8250	

[a]PRESS, predicted residual sum of square.

Table 7
ANOVA table (partial sum of squares) for response surface reduced quadratic model (Response: J_v)

Source	SS	DF	MS		F-value	p-value
Model	2.84E-10	4	7.11E-11		223.86	<0.0001 significant
X_1	9.7E-11	1	9.7E-11		305.41	<0.0001
X_2	1.48E-10	1	1.48E-10		465.86	<0.0001
X_1X_2	1.09E-11	1	1.09E-11		34.22	<0.0001
X_2^2	9.55E-12	1	9.55E-12		30.06	<0.0001
Residual	2.22E-11	70	3.18E-13			
Lack-of-fit	7.55E-12	20	3.78E-13		1.29	0.2318 not significant
Pure error	1.47E-11	50	2.94E-13			
Cor total	3.07E-10	74				
Standard deviation	5.64E-07		R^2		0.9275	
Mean	5.37E-06		Adjusted R^2		0.9233	
C.V.%	10.50		Predicted R^2		0.9165	
PRESS	2.56E-11		Adequate precision		50.58	

adequate signal and suggests that the model can be used in the range of the variables investigated.

A similar detail of analysis of the reduced quadratic model for flux rate is given in Table 7. The *F*-value of 223.86 and the corresponding "Prob. > *F*" (<0.0001) value indicate that the model is very significant. Further, the "Lack of Fit *F*-value" of 1.29 indicates that the lack of fit is not significant. For flux rate, the ranking of significant model terms were: the main effect of [MPDA] (X_2) > main effect of [TMC] (X_1) > the two-level interaction of [TMC] and [MPDA] (X_1X_2) > quadratic effect of [MPDA] (X_2^2). The interpretation of the other terms in the table is similar to the case of B discussed in the previous paragraph.

The regression equations in terms of coded factors were obtained for responses B and J_v are as follows:

$$B = 0.1010 - 0.0526X_1 + 0.0172X_2$$
$$- 0.042X_1X_2 + 0.0245X_1^2 + 0.0943X_2^2 \qquad (6)$$
$$- 0.0738X_1X_2^2 + 0.0211X_2^3$$

$$J_v = 4.7406 \times 10^{-6} - 1.653 \times 10^{-6}X_1$$
$$+ 2.0165 \times 10^{-6}X_2 - 7.823 \times 10^{-7}X_1X_2 \qquad (7)$$
$$+ 8.5295 \times 10^{-7}X_2^2$$

In terms of actual factors,

$$B = 0.6926 - 2.6626 \times [TMC] - 0.4614 \times [MPDA]$$
$$+ 2.0273 \times [TMC] \times [MPDA] + 1.5716 \times [TMC]^2$$
$$+ 0.071 \times [MPDA]^2 - 0.5908 \times [TMC] \times [MPDA]^2$$
$$+ 0.0211 \times [MPDA]^3$$
$$\qquad (8)$$

$$J_v = 4.2428 \times 10^{-6} - 7.045 \times 10^{-7} \times [TMC] - 3.001$$
$$\times 10^{-7} \times [MPDA] - 6.258 \times 10^{-6} \times [TMC] \times [MPDA]$$
$$+ 8.5295 \times 10^{-7} \times [MPDA]^2$$
$$\qquad (9)$$

These cubic and quadratic response functions were used to predict the intrinsic salt permeability and flux rate within the limits of experimental ranges.

The normal probability plot of the residuals, the plot of the residuals vs. the predicted response, and the plot of predicted vs. actual response are shown in Figs. 1–3, respectively. The points in Fig. 1 generally fall on a straight line implying that the errors were distributed normally, as assumed in the analysis. The scatter of residuals in Fig. 2 shows a satisfactory degree of randomness above and below the *x*-axis in general, implying that the proposed models were adequate and that the error variance was fairly constant. Fig. 3(a) and (b) compares the predicted responses (of B and J_v) vs. actual, and reveals a good agreement in the range of the operating variables. Fig. 3(c) is a parity plot between predicted and observed salt passage values, where the former was calculated from the predicted values for B and J_v, in accordance with Eq. (5). Understandably, the scatter here is more than either B or J_v alone (since the errors in both contribute to the error in salt passage), but in the region of low R_p values (which is the region of interest), the error is satisfactorily small.

Figs. 4 and 5, respectively, show 3D and surface contour plots for intrinsic salt permeability and flux rate. As seen from these figures, increases in [TMC] resulted in a reduction in intrinsic salt permeability and water flux. The membranes produced using
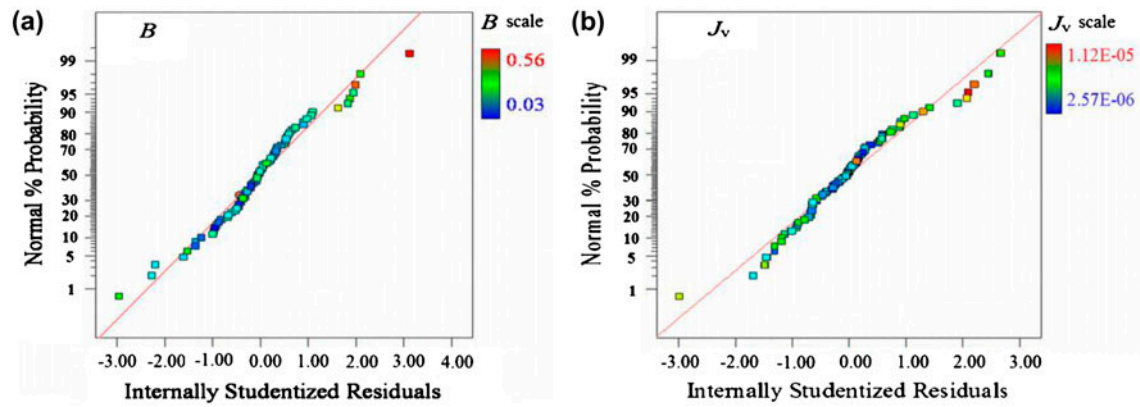
Fig. 1. The normal probability plot of the residuals for (a) intrinsic salt permeability and (b) water flux rate.
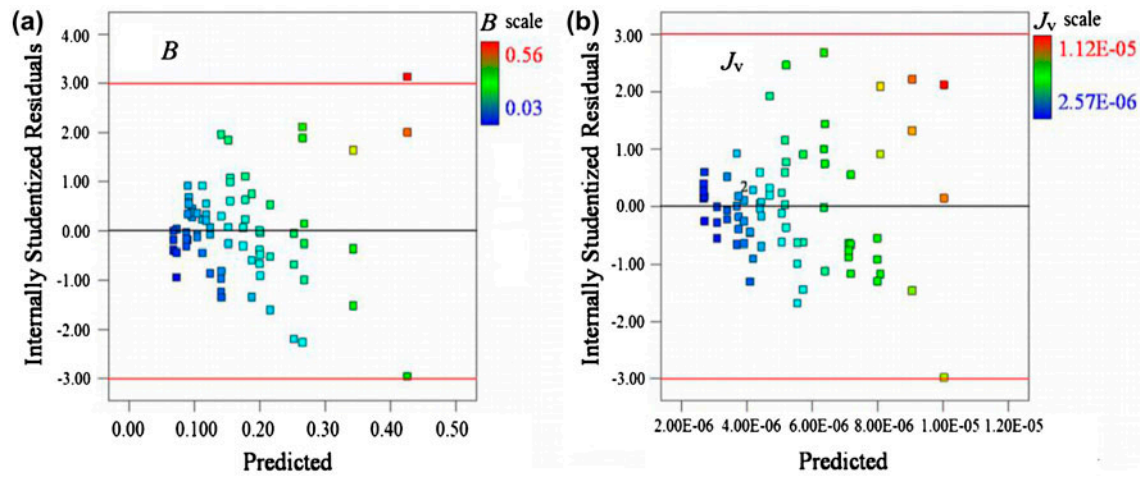

Fig. 2. The plot of the residuals vs. the predicted response for (a) intrinsic salt permeability and (b) water flux rate.
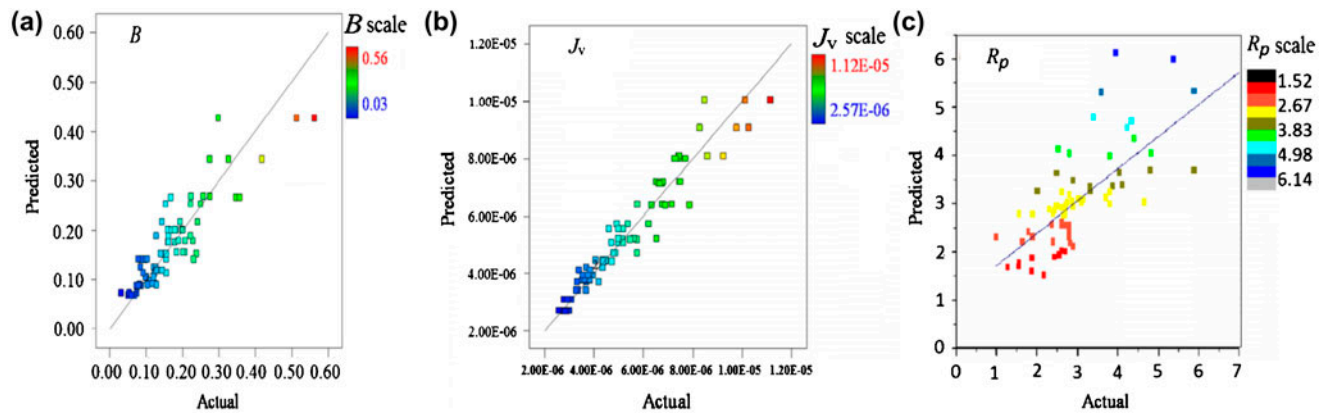

Fig. 3. Predicted vs. actual response for (a) intrinsic salt permeability (b) water flux rate, and (c) salt passage.
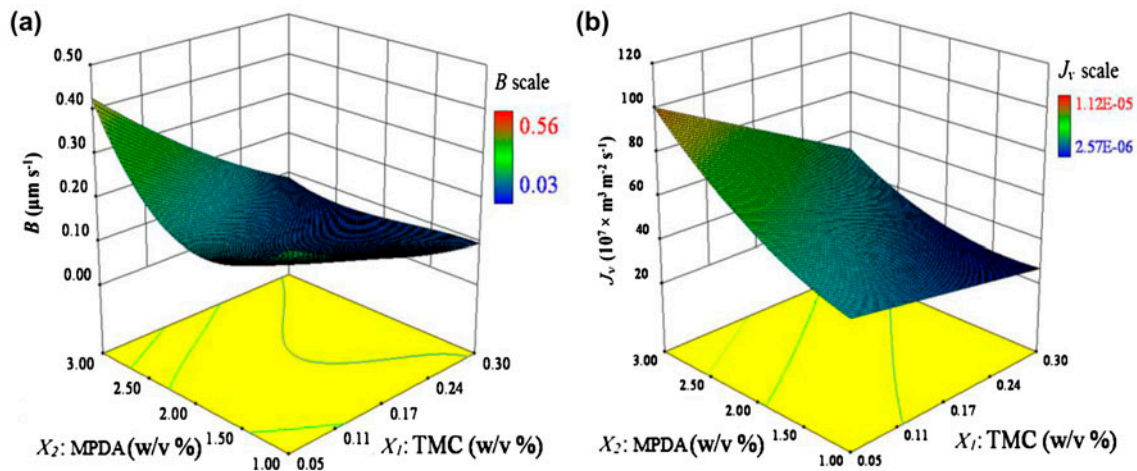
Fig. 4. 3D plot for (a) intrinsic salt permeability and (b) water flux rate.
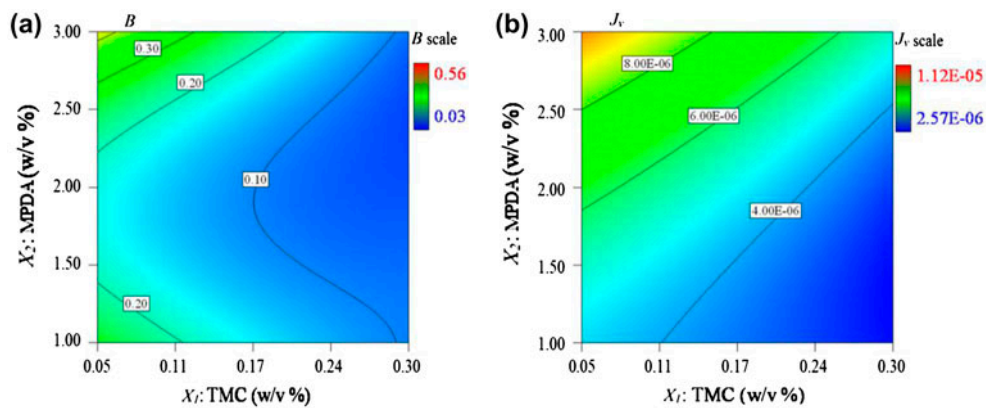

Fig. 5. Surface contour plot for (a) intrinsic salt permeability and (b) water flux rate.

[TMC] and [MPDA] in between 0.1–0.15 (w/v%) and 2–2.5 (w/v%), respectively, showed optimum properties in terms of intrinsic salt permeability (and hence salt passage) and flux rate. The surface contour plots in Fig. 5 can also be used to determine the combinations of [TMC] and [MPDA], which give the same values of response properties.

4.1.2. Confirmation runs

In order to confirm the model validity, five confirmation experiments were performed. Table 8 shows the preparation conditions, the experimental results, and the comparison with predictions from the models above. In view of practical importance, only results for salt passage and water flux are shown. Predictions of salt passage in this table were made from those of B and J_v using Eq. (5). While considering the

errors in salt passage predictions, therefore, it must be remembered that they are influenced by the errors in both B and J_v, and also in the terms of salt rejection (which is the normally used performance indicator), the error is small (0.06% at most). These results therefore indicate that the regression models obtained may be used with confidence to predict the performance of PA TFC membranes in the range of concentrations studied.

4.2. Analysis of membrane characteristics

In this section, we present the details of the effect of the concentrations of monomers on the various structural and physical attributes of the membranes. For the sake of brevity, only the salient conclusions from the statistical analysis are summarized and detailed tables are not presented.

Table 8
Confirmation runs

X_1 (w/v%)	X_2 (w/v%)	R_p (%)			J_v (10^7 m^3 m^{-2} s^{-1})		
		Actual	Predicted	Error (%)	Actual	Predicted	Error (%)
0.3	2.00	1.9	2.3	17.39	29.75	30.88	3.61
0.2	2.50	2.2	2.1	−4.76	48.5	55.53	12.71
0.15	1.00	4.1	4.5	8.88	37.86	37.51	−0.92
0.08	2.25	2.9	2.6	−11.53	66.19	67.03	1.23
0.13	2.25	1.7	2.3	26.08	52.08	59.63	12.67

Permeation across TFC–RO membrane is believed to occur by a solution-diffusion mechanism [24]. Since according to this model, permeability is inversely related to thickness, thickness (δ_m) of the PA layer and how it is influenced are important to understand. As noted earlier, membrane preparations for characterization studies were made separately from those used in the performance studies. For each membrane, at least five different samples were taken for PA thickness measurement. All the thickness values were statistically analyzed using repeated two-way ANOVA. Tests of significance showed that the difference in the mean thickness values among the different levels of TMC concentration was greater than would be expected by chance after allowing for effects of differences in MPDA concentration (and vice versa). The effect of the TMC concentration levels was independent of the level of MPDA concentration; there was no statistically significant interaction between TMC and MPDA levels.

Fig. 6(a) shows the mean effects of TMC and MPDA on PA film thickness. It is seen that, with an increase in TMC concentration the membrane thickness increased. At a given TMC level, an increase in MPDA concentration generally resulted in lower thickness values, although the effect was less pronounced as compared to the trend with [TMC]. Least square (LS) means for TMC showed that, in the optimum concentration window identified above, an increase in [TMC] from 0.05 to 0.3 (w/v%) resulted in an increase in thickness from 176.52 to 281.88 nm (at [MPDA] = 2 w/v%), and an increase in [MPDA] from 1 to 3 (w/v%) resulted in a decrease in thickness from 258.02 to 217.18 nm at [TMC] = 0.15 w/v%. Results in the literature on the dependence of film thickness on monomer concentrations, both theoretical and experimental, are very varied, and hence different mechanisms have been suggested. According to the mechanistic picture proposed by Freger and Srebnik [4], polymerization proceeds in the organic phase, with progressive increase in viscosity as crosslinking progresses leading finally to gelification and formation of the film. They found that the film thickness should decrease at constant [MPDA] as [TMC] is increased, contrary to our findings here, while their predictions on the effect of [MPDA] at constant [TMC] would be in agreement with our results. The variations in thickness in our case are due to the variations in conversion.
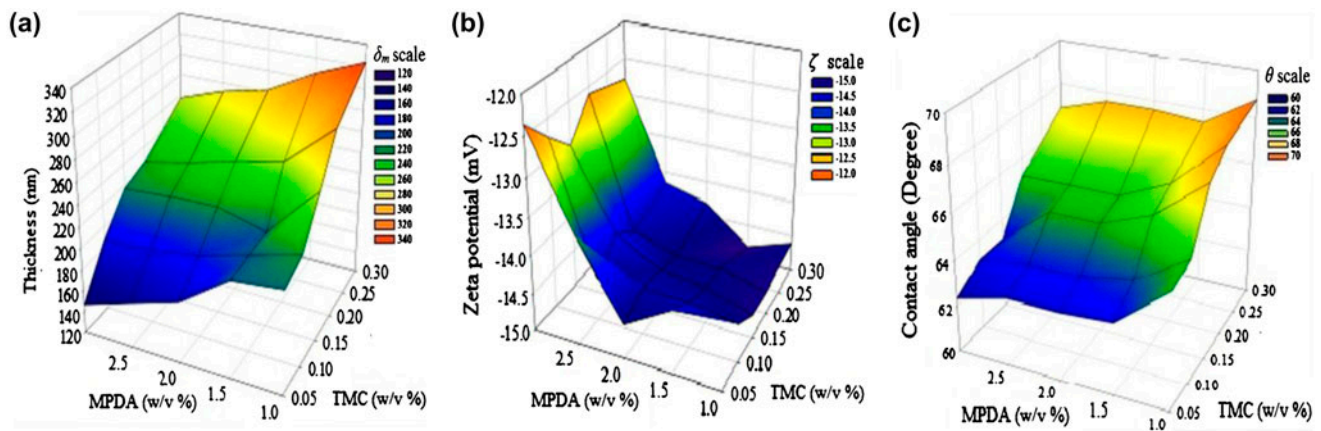

Fig. 6. Mean effect of TMC and MPDA concentration on (a) thickness, (b) zeta potential, and (c) contact angle of TFC membranes.

Conversion is limited by two factors: initial monomer concentrations that decide which monomer is stoichiometrically limiting, and the lowering of pH due to the hydrochloric acid (HCl) produced, which limits the availability of MPDA at the reaction locale. It is also possible that there is a competition between chain growth and crosslinking reactions, and at high concentrations of TMC (relative to MPDA), the balance tilts in favor of the chain growth reactions. This is reasonable as each molecule of TMC comes with two chain ends which contribute to growth, and only one side group which contributes to crosslinking. Thus, the gelification stage is postponed at high TMC concentrations, leading to thicker films. Thickness of the BW30 membrane was measured as 180 nm, which compares reasonably with our membranes when the larger roughness of our membranes is factored in.

In order to determine zeta potential (ζ), two sets of membrane samples were analyzed for each preparation condition. All the membranes showed a negative surface charge. The value of zeta potential for BW30 membrane was −14.89, in reasonable agreement with the TFC membranes prepared in this work.

The trends in the mean values are shown in Fig. 6(b). While on the whole, the variation in zeta potential was quite small, it is seen that at the highest value of [MPDA] employed, the zeta potential tends to less negative values than at the other concentra-tions. The influence of [TMC] is seen to be altogether negligible. These observations were confirmed by the statistical parameters, which in fact showed that over the whole range there was no statistically significant difference in the mean value among different concentration levels of TMC or MPDA. The interaction between these treatments was also not statistically significant, at a p-value of 0.786.

Contact angle shows the wettability of the polymer surface [25]. For each membrane, five different samples were analyzed to measure the contact angle with water. The trends in the mean values are shown in Fig. 6(c). The PSF support membrane showed an average contact angle (θ) of 91°, in comparison with which the contact angles with the PA layer are smaller, which indicates that the PA layer is relatively more hydrophilic than the support membrane. The contact angle for BW30 was measured as 41.6°, and the smoother surface of the membrane may be partly responsible for this low value.

A statistical analysis of the results on contact angle showed that the difference in the mean values among the different levels of TMC or MPDA was greater than would be expected by chance after allowing for effects of differences in MPDA or TMC concentration levels. There was a statistically significant difference ($p < 0.001$). On the other hand, the interaction between the two factors was not significant, at a p-value of
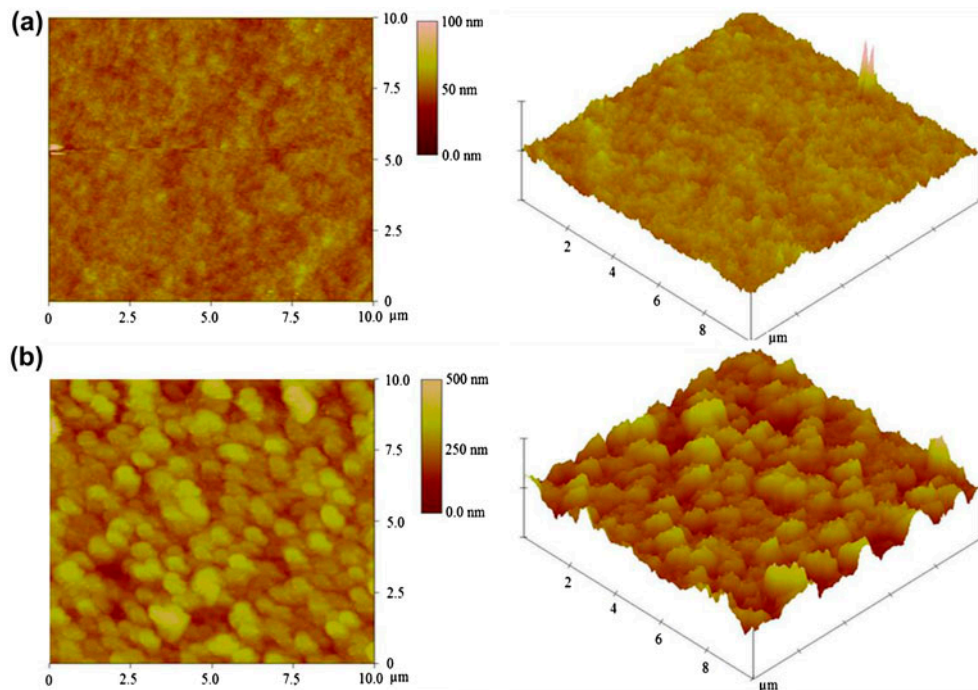

Fig. 7. AFM images of (a) PSF support and (b) BW30 membrane.

0.066. The hydrophilic character of the polyamide membrane has contributions from reacted and residual hydrophilic functional groups, the concentration and relative proportions of which depend on TMC and MPDA concentrations [26]. Fig. 6(a) and (c) shows that the trends in contact angle parallel somewhat to the trends in thickness are discussed earlier. Also as in the case of thickness, the effect of [MPDA] was much smaller over the range investigated as compared to that of [TMC]. It was seen that for 2 (w/v%) MPDA, varying the TMC concentration from 0.05 to 0.3 (w/v%), the contact angle increased from 62.92° to 67.6°. As pointed out by Freger and Srebnik [4], hydrophilicity/hydrophobicity considerations have to also factor in the differences in roughness. While this can be done to examine any correlation between hydrophilicity and performance in the present case,

relating hydrophilicity with preparation conditions is more questionable since the laboratory preparations are carried out in the absence of any fluid shear, which in the case of large scale manufacture, could influence the surface roughness of the PA layer produced. Differences in contact angle seen in the present case are thus possible due to (i) an increase in the –NH_2 chain ends at high [MPDA], and (ii) changes in roughness caused by the differences in local reaction rates in the absence of any fluid shear.

To study the roughness profiles of the membranes using AFM, eight different [TMC]–[MPDA] combinations (all five [MPDA] concentrations at [TMC] = 0.1 w/v%, and [TMC] of 0.05, 0.2, and 0.3 w/v% at [MPDA] = 2 w/v% were selected, along with commercial BW30 and polysulfone support membrane. Fig. 7(a) and (b) shows, respectively, the AFM scan
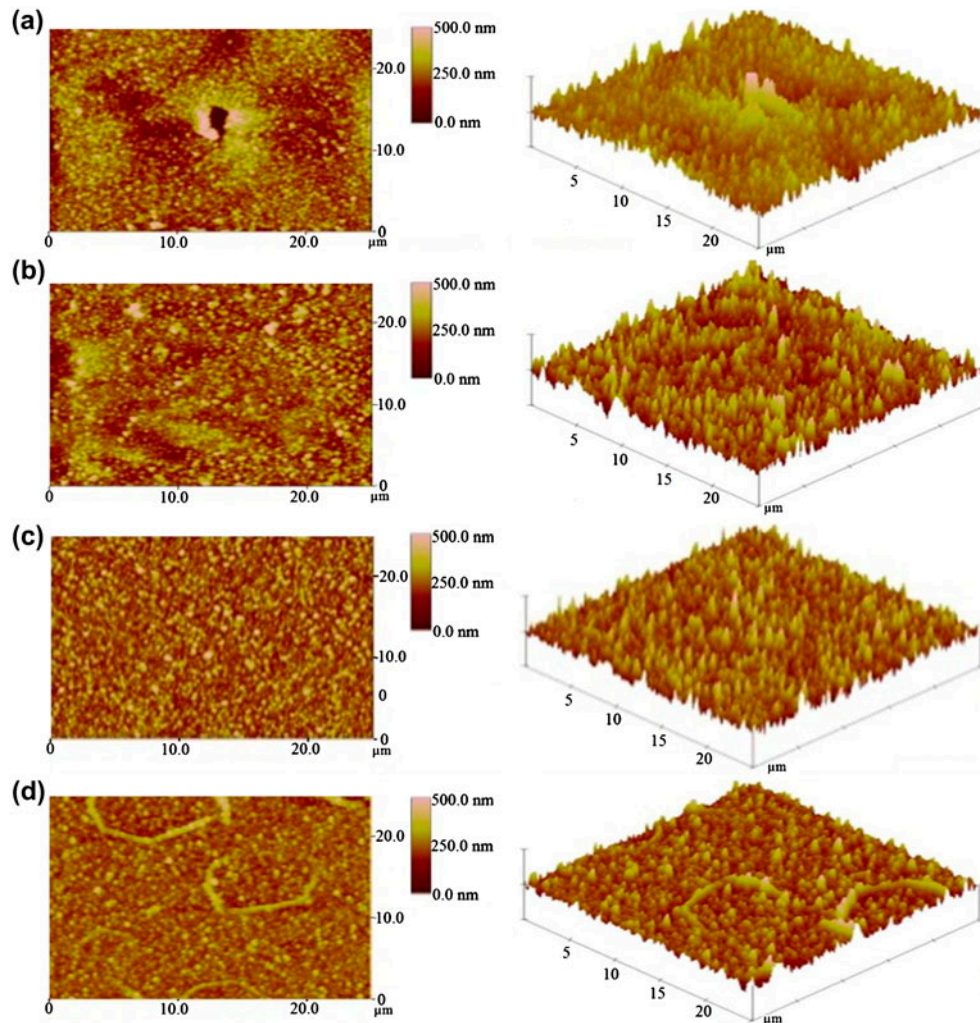

Fig. 8. 2D, 3D, and AFM images of laboratory prepared TFC membrane from TMC/MPDA concentration of (a) 0.05/2.0; (b) 0.3/2.0; (c) 0.1/1.0; and (d) 0.1/3.0.
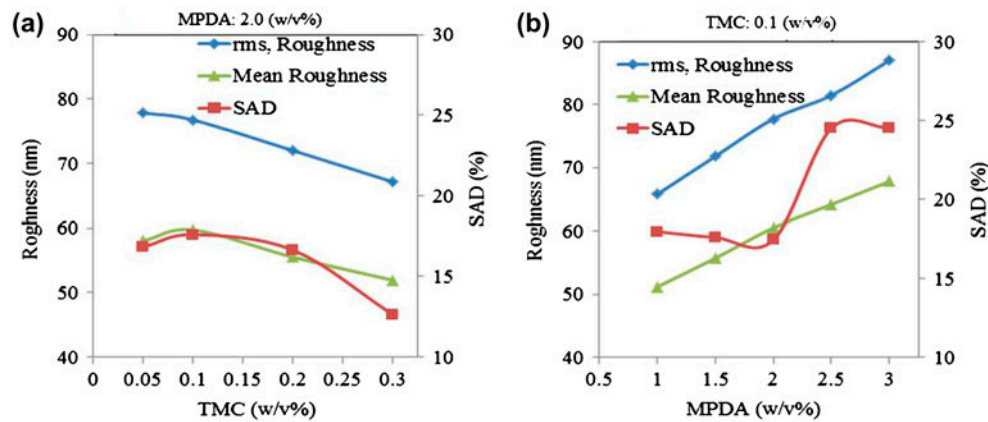
Fig. 9. Effect of (a) TMC and (b) MPDA concentration on membranes roughness properties.
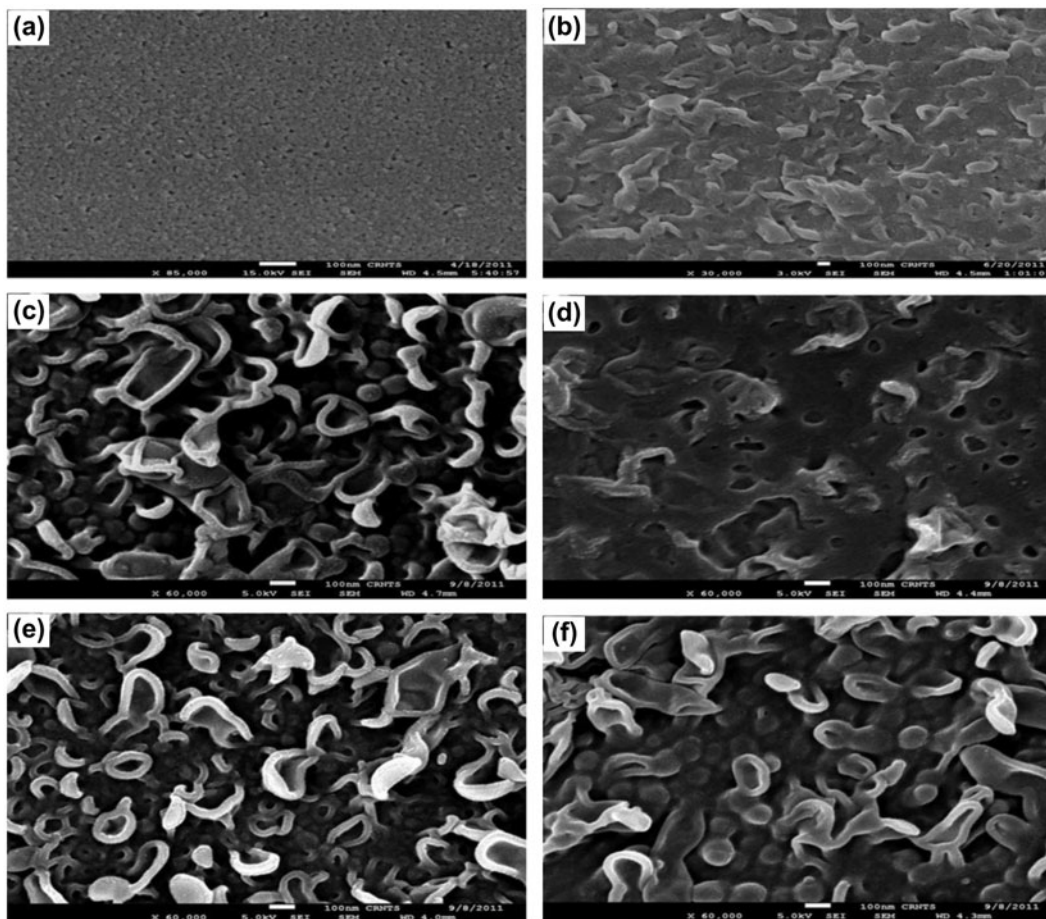

Fig. 10. Surface SEM microstructure of (a) PSF support (b) BW30, and TFC membranes from TMC/MPDA concentration of (c) 0.05/2.0; (d) 0.3/2.0; (e) 0.1/1.0; and (f) 0.1/3.0.

results for the support polysulfone membrane and the BW30 membrane, while Fig. 8 compares the surface features of four of the membranes made in the present study. While a rough "ridge-and-valley" surface morphology of TFC membranes is seen in general, membranes made in this study (Fig. 8) are seen to be

Table 9
Correlations among performance parameters structure/morphological characteristics

Correlation coefficient	B (µm/s)	J_v (m/s)	δ_m (nm)	θ (°)	ζ (mV)	RMS (nm)	SAD (%)
SAD	0.77	0.83	−0.69	−0.67	0.57	0.79	1
RMS	0.68	0.96	−0.74	−0.78	0.64	1	
ζ	0.62	0.76	−0.45	−0.42	1		
θ	−0.66	−0.82	0.94	1			
δ_m	−0.69	−0.80	1				
J_v	0.78	1					
B	1						

rougher than the commercial BW30. This is possibly the effect of fluid shear during the commercial membrane formation process. Further, commercial membrane manufacturing process could have used additives such as a surfactant in the aqueous phase, which could lower the interfacial tension between the two immiscible phases, a factor which might also influence surface roughness. The statistical difference in the root mean squared (RMS) roughness values among the treatment groups were greater than would be expected by chance ($p < 0.001$). The variation in RMS roughness is represented in Fig. 9. The surface roughness and surface area difference (SAD) decreased with an increase in [TMC] at [MPDA] = 2 (w/v%) (Fig. 9(a)), and with a decrease in [MPDA] at [TMC] = 0.1 w/v% (Fig. 9(b)). Thus, prepared TFC membranes appeared to have more rough surface than commercial BW30 (RMS 40.25 nm and SAD 10.9%) and polysulfone support membrane (RMS 4.6 nm and SAD 0.5%) (Fig. 7).

Surface microstructure of TFC membranes, for the same eight samples examined under the AFM, were also studied by FEG-SEM as shown in Fig. 10. Fold like protuberances and asperities typical of the polyamide layer in TFC membranes were prominently seen on the membrane surface. The density of such features decreased with an increase in [MPDA]. However, the individual features were more prominent at higher [MPDA]. In case of higher [TMC], the surface appeared smoother than lower [TMC].

4.3. Correlations between structure and function

It is clear from the results that in the concentration space investigated, the variation in zeta potential is marginal, and that in contact angle moderate, while variations in thickness are significant. It would be interesting to see which of the attributes correlates best with membrane function. Table 9 examines the correlations between membrane performance parameters and the structure/morphological features studied here. In this table, the number at the intersection of a column and a row gives the correlation between the respective parameters. The fairly good correlation between B (all coefficients above 60%) and J_v (all coefficients above 75%) on the one hand, and each of the membrane characteristics examined on the other hand, is interesting and shows the important role the structure plays in determining the performance. A good correlation between contact angle and roughness is also noteworthy and suggest that in laboratory preparations of the type adopted here (and in similar studies in the literature), the two cannot usually be varied independently.

5. Conclusions

A series of TFC membranes were prepared by IP reaction over five different MPDA and TMC concentrations in order to establish the effect of monomer concentration on the structure and properties of such membranes, within the range of practical interest. Structural properties and desalination performance of these membranes were systematically evaluated, and the data were statistically analyzed. The results indicate the predominant role preparation conditions in determining the performance of such membranes and strongly suggest the structural/morphological parameters important in determining performance. TMC and MPDA treatments showed significant effect on responses R_p, B, and J_v. The salt passage and water flux values of the membranes prepared in this work ranged from 0.99 to 7.4% and 25.7×10^{-7} to 111.6×10^{-7} m^3 m^{-2} s^{-1}, respectively. The trend for the simple mean effect of TMC for B at different [MPDA] levels was $1.5\% < 2\% < 2.5\% < 1\% < 3\%$, while for J_v, it was $1\% < 1.5\% < 2\% < 2.5\% < 3\%$. Further, within the limits of experimental factors, RSM analysis showed the reduced cubic model and quadratic model as significant for B and J_v, respectively. The model was further validated using diagnostic experiments. The mean effect and contour surface plots showed that the membranes produced using [TMC] and [MPDA] in between 0.1–0.15 and 2–2.5 (w/v%), respectively,

showed optimum properties in terms of B, R_p, and J_v. Within the range of concentrations studied, the variations observed in the thickness of PA layer were significant. An increase in [TMC] from 0.05 to 0.3 (w/v%) led to an increase in membrane thickness from 176.52 to 281.88 nm/for[MPDA] = 2 (w/v%), while an increase in [MPDA] from 1 to 3 (w/v%) caused a decrease in thickness from 258.02 to 217.18 nm, for [TMC] = 0.15 w/v%. The membrane charge was only marginally affected by variations in monomer concentrations. Mean values of contact angle among the different levels of [TMC] or [MPDA] was greater than would be expected by chance. For 2 (w/v%) MPDA, varying the TMC concentration from 0.05 to 0.3 (w/v%), the contact angle increased from 62.92° to 67.6°. The surface roughness and SAD decreased with an increase in [TMC] at given [MPDA] = 2 (w/v%), and decreased with an increase in [MPDA] at given [TMC] = 0.1 w/v%. The surface microstructure appeared smoother at lower [TMC]. Correlation analysis showed the important role of the structural attributes in determining the performance parameters. It should thus be possible to tailor the structural characteristics, and hence the performance of TFC membranes according to end-use application by varying concentration of the membrane forming agents. With concentrations of the monomers in the optimum window, further improvements in desalination performance can be sought using different organic and inorganic additives along with MPDA and/or TMC solution.

Acknowledgments

References

[1] W.J. Lau, A.F. Ismail, N. Misdan, M.A. Kassim, A recent progress in thin film composite membrane: A review, Desalination 287 (2012) 190–199.

[2] S.S. Dhumal, A.K. Suresh, A comprehensive model for kinetics and development of film structure in interfacial polycondensation, Polymer 50 (2009) 5851–5864.

[3] S.S. Dhumal, A.K. Suresh, Understanding interfacial polycondensation: Experiments on polyurea system and comparison with theory, Polymer 51 (2010) 1176–1190.

[4] V. Freger, S. Srebnik, Mathematical model of charge and density distributions in interfacial polymerization of thin films, J. Appl. Polym. Sci. 88 (2003) 1162–1169.

[5] A.K. Ghosh, B.-H. Jeong, X. Huang, E.M.V. Hoek, Impacts of reaction and curing conditions on polyamide composite reverse osmosis membrane properties, J. Membr. Sci. 311 (2008) 34–45.

[6] A.L. Ahmad, B.S. Ooi, Properties–performance of thin film composites membrane: Study on trimesoyl chloride content and polymerization time, J. Membr. Sci. 255 (2005) 67–77.

[7] S.Y. Kwak, S.G. Jung, S.H. Kim, Structure–motion–performance relationship of flux-enhanced reverse osmosis (RO) membranes composed of aromatic polyamide thin films, Environ. Sci. Technol. 35 (2001) 4334–4340.

[8] S. Qiu, L. Wu, L. Zhang, H. Chen, C. Gao, Preparation of reverse osmosis composite membrane with high flux by interfacial polymerization of MPD and TMC, J. Appl. Polym. Sci. 112 (2009) 2066–2072.

[9] N.K. Saha, S.V. Joshi, Performance evaluation of thin film composite polyamide nanofiltration membrane with variation in monomer type, J. Membr. Sci. 342 (2009) 60–69.

[10] S. Yi, Y. Su, B. Qi, Z. Su, Y. Wan, Application of response surface methodology and central composite rotatable design in optimizing the preparation conditions of vinyltriethoxysilane modified silicalite/poly-dimethylsiloxane hybrid pervaporation membranes, Sep. Purif. Technol. 71 (2010) 252–262.

[11] A.F. Ismail, P.Y. Lai, Development of defect-free asymmetric polysulfone membranes for gas separation using response surface methodology, Sep. Purif. Technol. 40 (2004) 191–207.

[12] S.S. Madaeni, N. Arast, F. Rahimpour, Y. Arast, Fabrication optimization of acrylonitrile butadiene styrene (ABS)/polyvinylpyrrolidone (PVP) nanofiltration membrane using response surface methodology, Desalination 280 (2011) 305–312.

[13] M. Khayet, C. Cojocaru, M. Essalhi, Artificial neural network modeling and response surface methodology of desalination by reverse osmosis, J. Membr. Sci. 368 (2011) 202–214.

[14] F. Xiangli, W. Wei, Y. Chen, W. Jin, N. Xu, Optimization of preparation conditions for polydimethylsiloxane (PDMS)/ceramic composite pervaporation membranes using response surface methodology, J. Membr. Sci. 311 (2008) 23–33.

[15] M. Namvar-Mahboub, M. Pakizeh, Optimization of preparation conditions of polyamide thin film composite membrane for organic solvent nanofiltration, J. Chem. Eng. 31 (2014) 327–337.

[16] M.L. Lind, A.K. Ghosh, A. Jawor, X. Huang, W. Hou, Y. Yang, E.M.V. Hoek, Influence of zeolite crystal size on zeolite-polyamide thin film nanocomposite membranes, Langmuir 25 (2009) 10139–10145.

[17] W.E. Mickols, Composite membrane and method for making the same, in: US Patent No. 6337018 B1, Jan. 2002.

[18] J.-Y. Koo, J.-E. Kim,W.-J. Kimand K.S. Park, Composite polyamide reverse osmosis membrane and method of producing the same, in: US Patent No. 6245234 B1, June 2001.

[19] W.W. Hines, D.C. Montgomery, Probability and Statistics in Engineering and Management Science, third ed., Wiley, New York, NY, 1990.

[20] R.H. Myers, D.C. Montgomery, Response Surface Methodology, Wiley, New York, NY, 1995.

[21] J.M. Gohil, A.K. Suresh, Development of high flux thin-film composite membrane for water desalination: A statistical study using response surface methodology, Desalin. Water Treat. 52 (2014) 5219–5228.

[22] K.D. Broota, Experimental Design in Behavioural Research, New Age International (P) Ltd Publishers, New Delhi, 2003.

[23] A. Idris, F. Kormin, M.Y. Noordin, Application of response surface methodology in describing the performance of thin film composite membrane, Sep. Purif. Technol. 49 (2006) 271–280.

[24] Y. Jin, W. Wang, Z. Su, Spectroscopic study on water diffusion in aromatic polyamide thin film, J. Membr. Sci. 379 (2011) 121–130.

[25] M. Morra, E. Occhiello, F. Garbassi, Knowledge about polymer surfaces from contact angle measurements, Adv. Colloid Interface Sci. 32 (1990) 79–116.

[26] Y. Jin, Z. Su, Effects of polymerization conditions on hydrophilic groups in aromatic polyamide thin films, J. Membr. Sci. 330 (2009) 175–179.